The EMBO Journal (2013) 32, 2407–2417
www.embojournal.org

SOURCE DATA | TRANSPARENT PROCESS

THE EMBO JOURNAL

Mobilization of a plant transposon by expression of the transposon-encoded anti-silencing factor

Yu Fu[1,2], Akira Kawabe[3], Mathilde Etcheverry[4], Tasuku Ito[1,5], Atsushi Toyoda[6], Asao Fujiyama[6], Vincent Colot[4], Yoshiaki Tarutani[1,2] and Tetsuji Kakutani[1,2,5,*]

[1]Department of Integrated Genetics, National Institute of Genetics, Shizuoka, Japan, [2]Department of Genetics, School of Life science, The Graduate University for Advanced Studies (SOKENDAI), Shizuoka, Japan, [3]Department of Bioresource and Environmental Sciences, Faculty of Life Sciences, Kyoto Sangyo University, Kyoto, Japan, [4]Institut de Biologie de l'Ecole Normale Supérieure (IBENS), Centre National de la Recherche Scientifique (CNRS), UMR 8197, Institut national de la santé et de la recherche médicale (INSERM), U1024, Paris, France, [5]Department of Biological Sciences, Graduate School of Science, The University of Tokyo, Hongo, Tokyo, Japan and [6]Center for Genetic Resource Information, National Institute of Genetics, Shizuoka, Japan

Transposable elements (TEs) have a major impact on genome evolution, but they are potentially deleterious, and most of them are silenced by epigenetic mechanisms, such as DNA methylation. Here, we report the characterization of a TE encoding an activity to counteract epigenetic silencing by the host. In *Arabidopsis thaliana*, we identified a mobile copy of the *Mutator*-like element (*MULE*) with degenerated terminal inverted repeats (TIRs). This TE, named *Hiun* (*Hi*), is silent in wild-type plants, but it transposes when DNA methylation is abolished. When a *Hi* transgene was introduced into the wild-type background, it induced excision of the endogenous *Hi* copy, suggesting that *Hi* is the autonomously mobile copy. In addition, the transgene induced loss of DNA methylation and transcriptional activation of the endogenous *Hi*. Most importantly, the *trans*-activation of *Hi* depends on a *Hi*-encoded protein different from the conserved transposase. Proteins related to this anti-silencing factor, which we named VANC, are widespread in the non-TIR *MULE*s and may have contributed to the recent success of these TEs in natural *Arabidopsis* populations.

The EMBO Journal (2013) **32,** 2407–2417. doi:10.1038/emboj.2013.169; Published online 30 July 2013
Subject Categories: chromatin & transcription; plant biology
Keywords: DNA methylation; epigenetics; evolution; transposon

Introduction

Control of transposable elements (TEs) has been extensively studied in plants. A pioneering early observation in maize is that TE activity often changes between active and inactive states in heritable but reversible manners (McClintock, 1951, 1958). The changes in the TE activity are generally correlated with the DNA methylation status; inactive TEs tend to be more methylated than active TEs (Chandler and Walbot, 1986; Brettell and Dennis, 1991; Fedoroff, 1996; Martienssen, 1996). The importance of DNA methylation in TE control has also been demonstrated using mutants of Arabidopsis; in Arabidopsis mutants with reduced genomic DNA methylation, a variety of silent TEs are de-repressed and mobilized (Miura *et al*, 2001; Singer *et al*, 2001; Kato *et al*, 2003; Lippman *et al*, 2004; Mirouze *et al*, 2009; Tsukahara *et al*, 2009).

Intriguingly, some TEs have mechanisms to counteract DNA methylation and silencing by the host. For example, McClintock's *Suppressor-mutator* (*Spm*) element in maize encodes a protein TnpA, which induces loss of DNA methylation in regions controlling transcript formation in *Spm* (Schläppi *et al*, 1994, 1996; Cui and Fedoroff, 2002). An active *Spm* transiently activates silent *Spm* copies *in trans*, a process likely to be mediated by TnpA (Cui and Fedoroff, 2002).

Robertson's *Mutator*, another well-characterized TE in maize, spontaneously changes its activity and DNA methylation in a coordinated manner (Chandler and Walbot, 1986; Martienssen and Baron, 1994; Martienssen, 1996). Like *Spm*, a silent *Mutator* element loses DNA methylation when an active *Mutator* is present in the same genome (Brown and Sundaresan, 1992; Lisch *et al*, 1995, 1999). *MuDR*, an autonomously mobile copy of maize *Mutator* family, contains two genes, *mudrA* and *mudrB*. The *mudrA* encodes the MURA protein, which is structurally similar to known transposases of other TEs (Eisen *et al*, 1994; Lisch, 2002). In addition, *mudrA* is sufficient for excision of *Mutator*, further suggesting that MURA functions as a transposase (Lisch *et al*, 1999). TEs similar to the maize *Mutator* are widespread in eukaryotes and they are referred to as *Mutator*-like elements (*MULE*s) (Jiang *et al*, 2004). ORFs related to *mudrA* are generally found in autonomous *MULE*s. Some of the autonomous *MULE*s also have additional ORF(s), such as *mudrB* in *MuDR*, but the structures of the proteins encoded in these ORFs are diverse and their functions remain largely unknown. In addition, some of the *MULE*s carry fragments of cellular genes, but their impacts on the TE dynamics and host fitness are still elusive (Talbert and Chandler, 1988; Yu *et al*, 2000; Jiang *et al*, 2004; Hoen *et al*, 2006).

Most of the class II (DNA-type) TEs have long terminal inverted repeat (TIR), but there are a few exceptions (Wicker, 2007). Although the maize *Mutator* elements have relatively long TIRs of almost identical sequences, subgroups of *MULE*s with extensively degenerated TIR have been found in the Arabidopsis genome and they are classified as non-TIR *MULE*s (Le *et al*, 2000; Yu *et al*, 2000). Although the theoretical sequence analyses of Arabidopsis genome suggest movement of these non-TIR *MULE*s in the past (Yu *et al*, 2000), direct evidence for *de novo* movements is limited (Hoen *et al*, 2006; Tsukahara *et al*, 2009).

We have previously reported that a group of non-TIR *MULE*s, called *VANDAL21*, seem to transpose in a back-

*Corresponding author. Department of Integrated Genetics, National Institute of Genetics, Yata 1111, Mishima, Shizuoka, Japan. Tel.: +81 55 981 6801; Fax: +81 55 981 6804; E-mail: tkakutan@lab.nig.ac.jp

Received: 14 March 2013; accepted: 4 July 2013; published online: 30 July 2013

ground of reduced genomic DNA methylation (Tsukahara *et al*, 2009). Here, we identified an autonomously mobile copy of *VANDAL21*, which we renamed *Hiun* (*Hi*). Despite the degeneration of TIRs, *Hi* is competent to excise and transpose in precise manners. Interestingly, a *Hi* transgene induced loss of DNA methylation, transcriptional activation, and excision of the endogenous *Hi* copy. Most importantly, these *trans*-acting effects of *Hi* do not depend on the protein related to MURA-type transposase but instead depend on another protein encoded by *Hi*. The function of this novel anti-silencing protein, which we named VANC, will be discussed in the context of TE evolution.

Results

Identification of mobile VANDAL21 copies

The genome sequence of wild-type Col (http://www.arabidopsis.org/) suggests seven copies of *VANDAL21* elements with relatively similar sequences. Other copies of *VANDAL21* are distant in the sequences. Consistent with that, Southern analysis revealed seven bands for that group of *VANDAL21* (Tsukahara *et al*, 2009). We have previously shown that additional bands emerge in Arabidopsis plants derived from several rounds of self-pollinations in *ddm1* (*decrease in DNA methylation 1*) mutant backgrounds, suggesting mobility of one or more copies of the *VANDAL21* members (Tsukahara *et al*, 2009). Arabidopsis *ddm1* mutation generally induces loss of DNA methylation in TEs, which causes mobilization of diverse TEs (Miura *et al*, 2001; Singer *et al*, 2001; Lippman *et al*, 2004; Mirouze *et al*, 2009; Tsukahara *et al*, 2009). In order to know which of *VANDAL21* copies are mobile, we used two methods: suppression PCR and whole-genome re-sequencing (see Materials and methods for details).

In total, we identified 72 *de novo* insertions of *VANDAL21*s (61 by genome re-sequencing and 14 by suppression PCR with 3 overlaps) in the self-pollinated *ddm1* lines (Supplementary Table S1). Of these 72 insertions, 69 correspond to one copy (Figure 1A; *AT2TE42810*) of *VANDAL21* element. The remain-

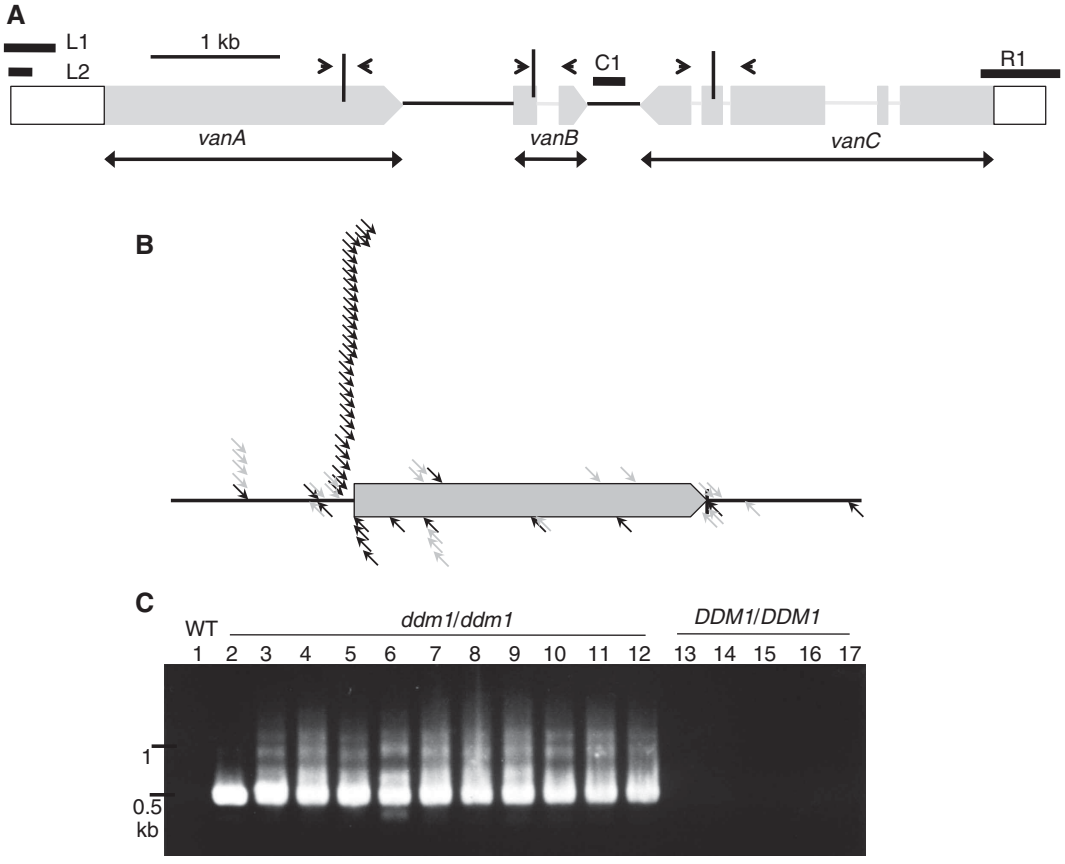

Figure 1 Mobilization of *Hi* in *ddm1* mutant. (**A**) Schematic diagram for structure of *Hi*. Terminal regions, exons, introns, and intergenic regions are shown by white bars, grey bars, grey lines, and black lines, respectively. Regions examined by bisulphite sequencing are shown by L1 and R1 with thick black lines. Region examined by McrBC-qPCR is shown by L2. Region examined for copy number quantification is shown by C1. In most of the transgene constructs, silent mutation is introduced for each ORF, so that the transcripts from the transgene and endogenous copy could be distinguished between. The sites of the silent mutations are shown by vertical bars, with surrounding arrowheads showing regions amplified by RT–PCR. Regions for ORFs deleted in each of the deletion constructs are shown by horizontal bars with two arrowheads. (**B**) *De novo* integration sites of *Hi* in relation to flanking transcription units. The position of integration is normalized by length of the flanking transcription unit. Rightward and leftward arrows indicate insertions with 5′ to 3′ and 3′ to 5′ orientations of *Hi*, respectively. Insertions flanking pseudogenes and transposon genes are shown by grey arrows, and those flanking canonical genes by black arrows. Sequences of the integration sites are shown in Supplementary Table S1. Four out of the sixty-nine insertions are not included in this figure, because they are further away from transcription units. Genomic locations of all 69 transpositions are shown in Supplementary Figure S2. (**C**) Excision of *Hi* in *ddm1* plants detected by PCR. Genomic DNA of 11 *ddm1* plants (lane numbers from 2 to 12) and 5 wild-type sibling plants (lane numbers from 13 to 17) was used to analyse excision of endogenous *Hi* by nested PCR. These lines are derived from segregating population in self-pollinated progeny of a *DDM1/ddm1-1* heterozygote. Sequences of primers used are shown in Supplementary Table S2. Source data for this figure is available on the online supplementary information page.

ing three insertions correspond to another copy (*AT4TE15615*). For the other five copies of related *VANDAL21*, no new insertion has been identified. In the following parts, we concentrate on the most active copy, *AT2TE42810*, which we renamed *Hiun* (*Hi*, Japanese for 'a flying cloud').

Structure of Hi

Hi is 8177-bp long and includes three ORFs: *At2g23500*, *At2g23490*, and *At2g23480* (Figure 1A). One ORF (*At2g23500*; called *vanA*) encodes a protein with high sequence similarities with MURA-type transposases, which are generally found in *MULE*s. Proteins encoded by two other ORFs (*vanB* and *vanC*) do not have sequence similarity to any characterized proteins. An unorthodox feature is that, unlike other typical mobile DNA-type TEs, the TIRs of this TE are extensively degenerated (Supplementary Figure S1A), showing the characteristics of non-TIR *MULE*s (Yu *et al*, 2000).

Integration and excision of Hi

Hi is transposed throughout the genome, although insertions may be more concentrated near the original locus than in unlinked regions (Supplementary Figure S2). *Mutator* elements in maize preferentially transpose into 5′ region of genes (Hardeman and Chandler, 1989; Dietrich *et al*, 2002; Liu *et al*, 2009). That was also the case for *Hi*; most of the integration sites are localized around transcription start sites of genes (Figure 1B). Interestingly, integration of *Hi* there had bias in the orientation (Figure 1B). Such a bias in the orientation has not been reported for the maize *Mutator* (Brown *et al*, 1989). The bias in the orientation of *Hi* integration might be related to the asymmetry in its terminal sequences. We could detect 9 bp of target site duplication (TSD) for most of the insertions examined (Supplementary Figure S1B), as is the case for integrations of other *MULE*s (Yu *et al*, 2000).

Many DNA-type TEs often transpose with loss of the original copy. Because *Hi* does not have typical structure of DNA-type TE, an interesting question would be whether *Hi* excision occurs at defined termini or not. In order to detect somatic excision events, we used PCR with primers for both of the flanking regions of the original *Hi* locus (details in Materials and methods). Using this assay, we could detect *Hi* excision in all independent *ddm1* lines examined (Figure 1C). We examined the mode of the excisions by sequencing the PCR products (Supplementary Figure S3A). Interestingly, despite the degeneration of TIRs, many of the excision products showed excision around the terminal sites predicted from the integrated copies. Even TSDs are lost in a significant part of the excision product.

In summary, these observations suggest that long perfect TIRs are dispensable not only for integration, but also for reasonably precise excision of this element in the defined termini. The transposition of *Hi* occurred in a manner comparable to that of typical *MULE*s with long TIR.

Mobilization of endogenous Hi by transgene

As the *ddm1* mutation results in transcriptional de-repression of many repeat sequences (Lippmann *et al*, 2004; Tsukahara *et al*, 2009), it is formally possible that mobilization of *Hi* in *ddm1* is triggered by de-repression of other sequence(s). In order to test if expression of proteins encoded by *Hi* is sufficient for its mobilization, we introduced a cloned *Hi* copy into wild-type plants by Agrobacterium-mediated transformation. In these transgenic *Hi* lines, we could detect transcripts corresponding to their three ORFs (Supplementary Figure S4). In these lines, the *Hi* transgene induced excision of the original copy (Figure 2A).

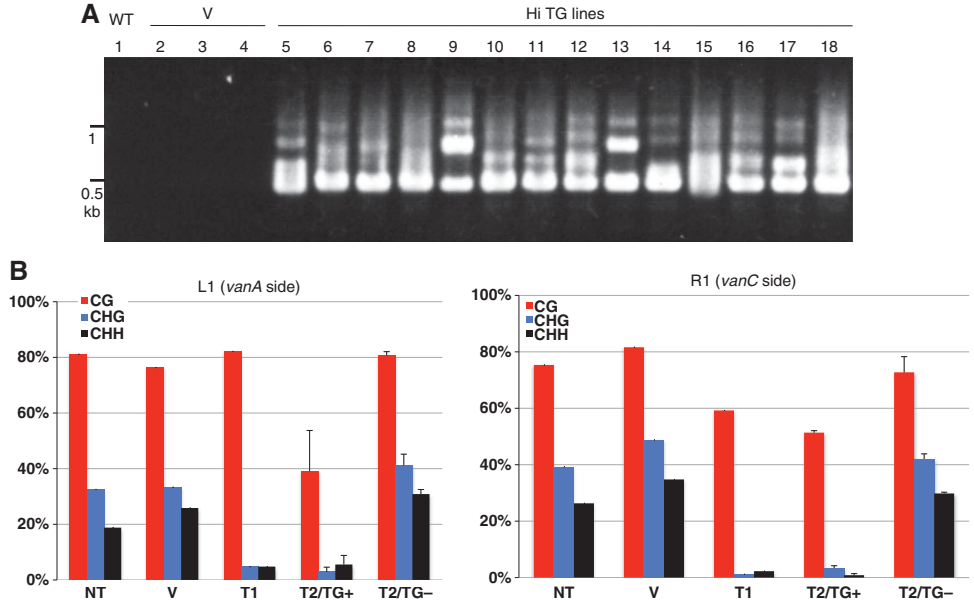

Figure 2 Introduction of *Hi* transgene induces loss of DNA methylation and excision of endogenous *Hi* copy. (**A**) Excision of endogenous *Hi* induced by transgene for *Hi* (*Hi* TG: lanes 5–18). Lanes 1 and 2–4 are non-transgenic plant (wt) and transformant lines with empty vector (V) used as negative controls, respectively. Excision of *Hi* copy in the transgene was also detected in some of the transgenic lines (Supplementary Figure S5). (**B**) DNA methylation status of *Hi* termini in the transgenic line and progeny. T1 transformant with *Hi* transgene showed reduction in DNA methylation in both termini, compared to non-transgenic plant (NT) and transformants with empty vector (V). T2/TG + and T2/TG − are self-pollinated progeny of the T1 with and without transgene, respectively. In both classes, averages and standard deviations of three segregants are shown. We also obtained essentially the same results for a segregating T3 family (Supplementary Figure S7). Regions L1 (upstream of *vanA*) and R1 (upstream of *vanC*) were examined (shown in Figure 1). At least 11 clones were examined for each plant. Source data for this figure is available on the online supplementary information page.

Control transformants with empty vectors did not show excision of the *Hi*, confirming that *Hi* transgene triggered mobilization of the endogenous copy. We also examined *Hi* activity in self-pollinated progeny of one of the *Hi* transgenic lines. We could detect *Hi* excision in most of 15 progeny plants that inherited the transgene (Supplementary Figure S6). On the other hand, we could not detect the excision in any of six progeny plants that lost the transgene by segregation, further confirming that the *Hi* transgene is responsible for the mobilization.

DNA demethylation induced by Hi in trans

The observations described above suggest that expression of *Hi* transgene induces mobilization of the endogenous copy. Interestingly, in the presence of the transgene, DNA methylation levels were reduced in both termini of the endogenous *Hi* (Figure 2B). The loss of methylation is more extensive in non-CpG sites than in CpG sites. When the transgene was segregated away in the self-pollinated progeny of the transgenic line (T2/TG − in Figure 2B), *Hi* was remethylated in the terminal regions, which was associated with its loss of excision activity.

We also tested the *trans*-acting demethylation effect for transposed *Hi* copies, using epi-Recombinant Inbred Lines (epi-RILs) from *ddm1* mutant (Johannes *et al*, 2009). The epi-RILs are originated from *ddm1* mutant backcrossed to parental wild-type Col to generate *DDM1/DDM1* homozygotes, and subsequent self-pollination to fix the heritable epigenetic defects induced by *ddm1*. The methylation status of *Hi* at the original locus was examined by PCR after digestion by methylation-sensitive restriction enzyme. As expected from the crossing scheme used to generate the

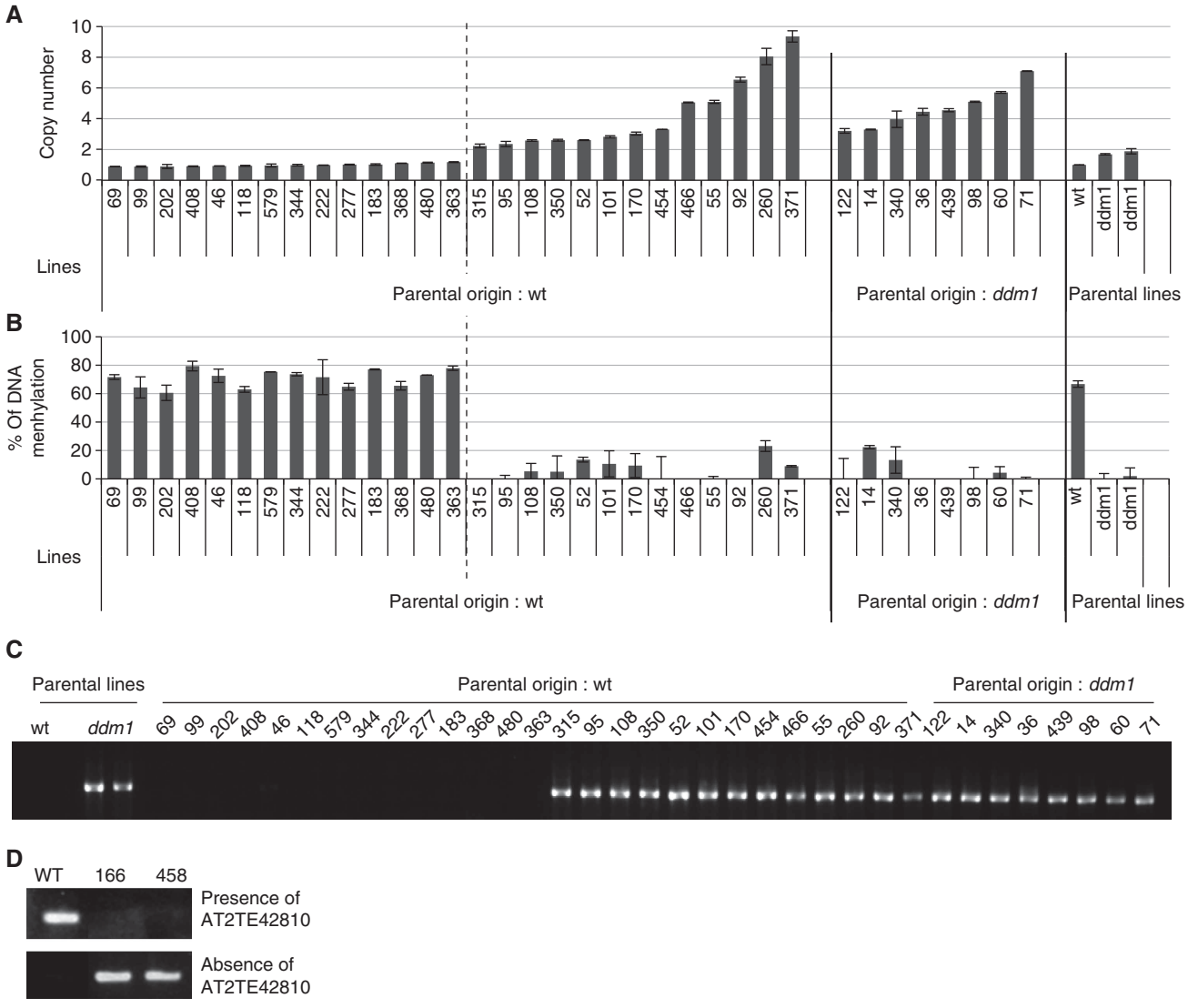

Figure 3 Transposed *Hi* induces loss of DNA methylation and excision of *Hi* in the original locus. (**A**) Copy number of *Hi* in each of the epi-RILs. The copy number was estimated by quantitative PCR using region C1 in Figure 1. Average and standard deviation of two technical replicates are shown in this and next panel. Parental origin of the original *Hi* locus (wt or *ddm1*) was determined by methylation status of the linked region (Colomé-Tatché *et al*, 2012). (**B**) DNA methylation status in the 5′ region (L2 in Figure 1) of the original *Hi* locus was estimated by McrBC digestion and subsequent qPCR. Details are described in Materials and methods. *Hi* in the original locus showed loss of DNA methylation when extra copies of *Hi* exist. (**C**) Excision analysis of original *Hi* copy by nested PCR. (**D**) Two of the epi-RILs showed germinal transmission of the excised *Hi* allele. Origin of the *Hi* locus is wild-type *DDM1* for line 166 and *ddm1* mutant for line 458. Presence of *Hi* in the original locus was examined by PCR in the 5′ border of *Hi* (the primer sequences are shown in Supplementary Table S2). Lack of the signal suggests fixation of the empty allele. Source data for this figure is available on the online supplementary information page.

epi-RILs (Johannes *et al*, 2009), approximately three quarters of the epi-RILs tested had inherited the original *Hi* copy from wild-type *DDM1* parent. Some of these lines have additional transposed *Hi* copies *in trans* (Figure 3A). In those lines, *Hi* at the original locus showed loss of methylation (Figure 3B), despite its wild-type origin. On the other hand, in epi-RILs that did not carry the additional *Hi*, *Hi* at the original locus remained methylated to the level comparable to parental wild type. Together, these results suggest that the stable demethylation of *Hi* at the original locus is due to *trans*-acting effect of the transposed *Hi* copies. In addition to its demethylation, the *Hi* copies present at the original locus showed excision (Figure 3C), and that happened only when the additional *trans*-acting copies exist. These *trans*-acting effects of the transposed *Hi* are consistent with the *trans*-acting demethylation and mobilization by the *Hi* transgene.

Expression of vanC is sufficient for the trans-activation and mobilization of endogenous Hi

The results shown above demonstrate that *Hi* transgenes induced mobilization of endogenous copy *in trans*, which is associated with loss of DNA methylation in the terminal regions. In order to further dissect the role for each of the ORFs in *Hi*, we generated transgenes with deletion in each ORF. Transgene with deletion of the central small ORF (*vanB*) still caused loss of methylation in both termini of *Hi* (Figure 4). By contrast, deletion of 3′ ORF (*vanC*) abolished the demethylation effect for both termini, suggesting that this ORF is essential for the demethylation. Transgene with deletion of 5′ ORF (*vanA*), which is structurally similar to transposase, still caused loss of methylation in 3′ (*vanC* side) terminal region of *Hi*, although the demethylation effect in the 5′ (*vanA* side) region was less complete than that in the full-length *Hi* transgenic lines. These results suggest that *vanC* is important for the demethylation of both of the terminal regions.

We then examined the effect of these deletion constructs on excision of endogenous copies (Figure 5A). Very importantly, transgenic lines with deletion in *vanA* (Δ*A*-TG) still induced excision of endogenous *Hi* (Figure 5A). This was surprising because *vanA* encodes the putative transposase. We then examined expression of endogenous *vanA* gene in the presence of Δ*A*-TG. In most of the Δ*A*-TG lines, endogenous *vanA* was de-repressed and transcribed, although the expression level was generally lower and less robust than that of the *Hi* transgene keeping *vanA* (Figure 5B; Supplementary Figure S8).

The results above suggest that expression of *vanB* and/or *vanC* can cause de-repression of *vanA*. We could also detect expression of *vanB* in Δ*B*-TG lines, but *vanC* transcript was undetectable in Δ*C*-TG lines (Supplementary Figure S8), suggesting possible role of *vanC* in the *trans*-activation. In addition, deletion of *vanB* from the transgene did not affect excision of endogenous *Hi* by the transgene, while the excision tended to be less robust in Δ*C*-TG (Figure 5A; Supplementary Figure S9). In order to know if *vanB* is dispensable for the *trans*-activation of *Hi*, we examined the effect of transgene with deletion of both *vanA* and *vanB* (Δ*AB*-TG). Only the *vanC* ORF remains in the Δ*AB*-TG construct. The Δ*AB*-TG also induced demethylation of 3′ (*vanC* side) terminal regions to the level comparable to the Δ*A*-TG (Figure 4). In most of the Δ*AB*-TG lines, we could detect excision of *Hi* and transcription of *vanA* and *vanB* (Figure 6A and B). In T2 generation that originated from self-pollination of a T1 Δ*AB*-TG plant, all T2 plants with the transgene showed excision, but none of T2 plants without transgene showed excision, confirming that the Δ*AB* transgene induces the excisions of endogenous *Hi* (Figure 6C). Taken together, these results demonstrate the key role of *vanC* for the *trans*-acting anti-silencing of *Hi*.

Proteins related to the anti-silencing factor are widespread in non-TIR MULEs but not found in TIR MULEs

Non-TIR *MULE*s in *A. thaliana* genome are consisted of multiple *VANDAL* and *ARNOLD* families (Yu *et al*, 2000; Figure 7A). Interestingly, the non-TIR *MULE*s seem to be very successful in the recent proliferation. The phylogenetic analyses revealed recent proliferations in multiple subfamilies of non-TIR *MULE*s; each of the subfamilies shows terminal proliferations after separation of *A. thaliana* and *A. lyrata* lineages. The proliferation rates of the non-TIR *MULE* clusters are significantly higher than those of TIR-*MULE* in both *A. thaliana* and *A. lyrata* lineages (Figure 7A; Table I).

Notably, all major branches of these proliferating non-TIR *MULE*s contain TEs with ORFs encoding proteins similar to the anti-silencing factor VANC (protein product of

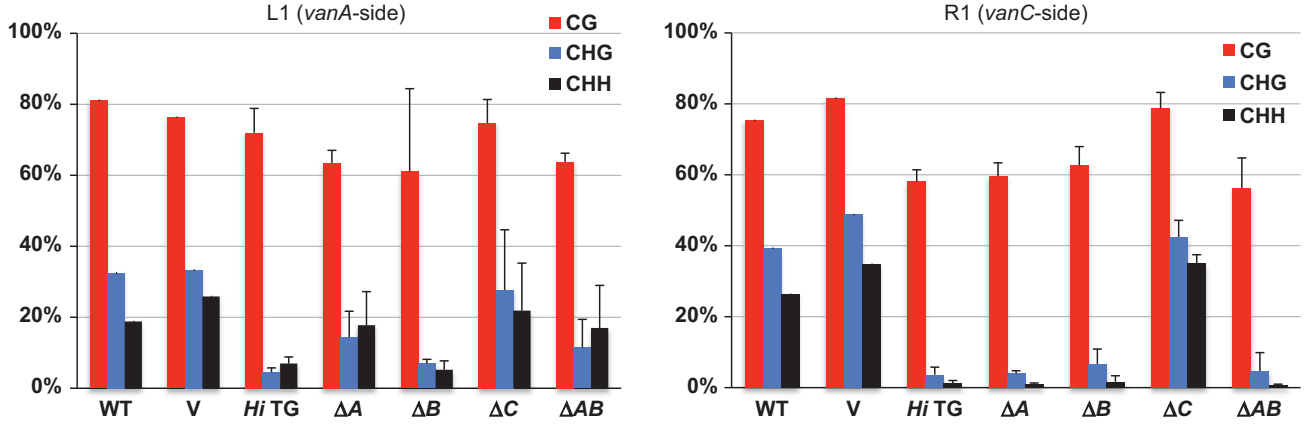

Figure 4 DNA methylation status of endogenous *Hi* after introduction of *Hi* transgene and its deletion derivatives. For each of the deletion derivatives, averages and standard deviations of four independent transgenic plant lines are shown. WT and V are from Figure 2.

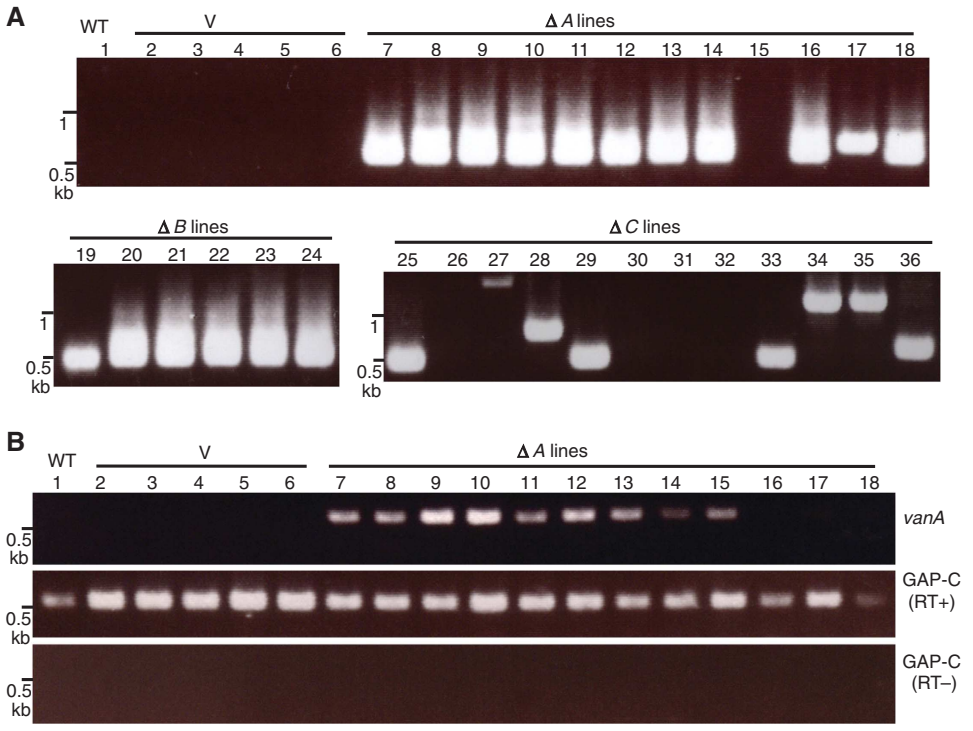

Figure 5 *Trans*-activation by *Hi* transgene without putative transposase. (**A**) Excision of endogenous *Hi* induced by Δ*A* transgene. Lanes 1 and 2–6 are non-transgenic plant (wt) and transformant lines with empty vector (V) used as negative controls, respectively. Excision of endogenous *Hi* induced by Δ*B* and Δ*C* transgene is also shown below. The results using additional Δ*C* lines are shown in Supplementary Figure S9. (**B**) Transcriptional activation of *vanA* induced by Δ*A* transgene. Materials for the same lane number in (**A**) and (**B**) are from the same plant, although the DNA and RNA are prepared from different leaves. Source data for this figure is available on the online supplementary information page.

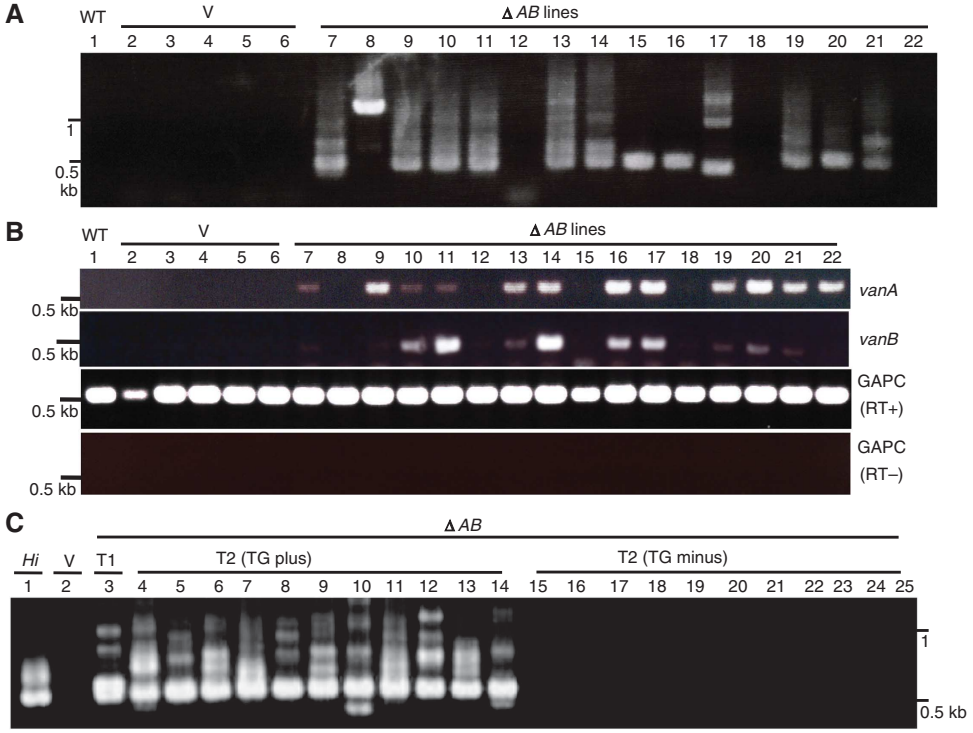

Figure 6 Expression of *vanC* is sufficient for the *trans*-activation. (**A**) Excision of endogenous *Hi* induced by Δ*AB* transgene. (**B**) Transcriptional activation of *vanA* and *vanB* genes induced by Δ*AB* transgene. Materials for the same lane number in (**A**) and (**B**) are from the same plant, although the DNA and RNA are prepared from different leaves. (**C**) Excision of endogenous *Hi* induced by Δ*AB* transgene in the T2 generation. T2 plants from self-pollinated progeny of a T1 (the plant shown in lane 9 of **A**) were examined after determining the presence/absence of the transgene. Source data for this figure is available on the online supplementary information page.

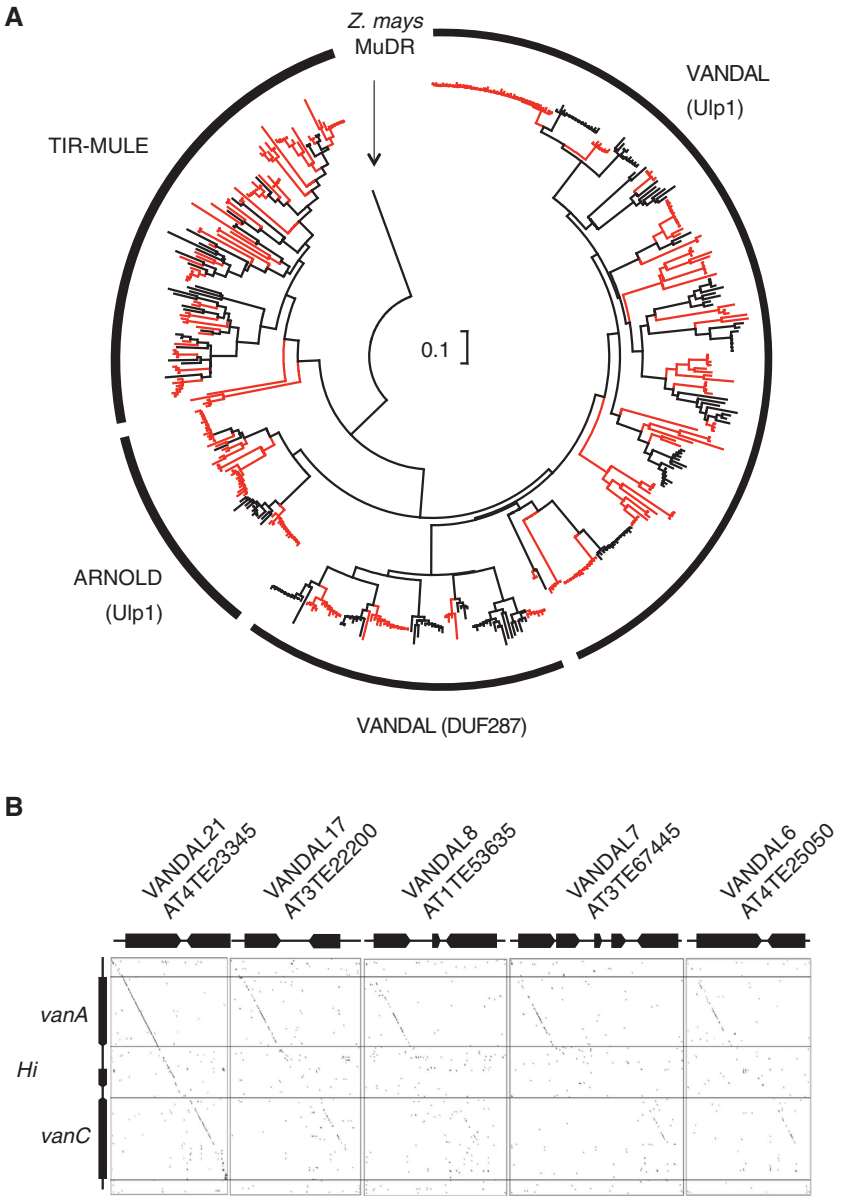

Figure 7 Evolution and proliferation of TIR and non-TIR *MULE* families. (**A**) Phylogenetic relationship among *MULE* families in genomes of *A. thaliana* and *A. lyrata*. *A. lyrata*-specific lineages are shown by red lines. An NJ tree made by *p*-distance is shown. Scale bar is shown in the centre of the tree. The families containing DUF287 or Ulp1 protease domain are indicated in the parentheses. Names of *VANDAL* members are shown in phylogenetic tree in Supplementary Figure S10. (**B**) Dot-plot (Harr-plot) analyses among *VANDAL* families. Regions with nucleotide identities of 15 out of 20 or more are shown by dots. Copies with typical structure were chosen from *VANDAL21*, *17*, *8*, *7* and *6* families. From *VANDAL21* family, one sequence each from two clusters was used. Coding regions are indicated by pointed thick lines.

vanC). All the VANC-related proteins contain the domain DUF1985 (domain of unknown function; Supplementary Figure S11). Some of them, including VANC, also contain the domain DUF287 (Figure 7; Supplementary Figure S11). Other *VANDAL* members, as well as *ARNOLD* members, have ORFs encoding Ulp1 proteases (Figure 7A; Supplementary Figure S11). Both the Ulp1 and DUF287 types of proteins contain DUF1985, generating a wide distribution of VANC-related proteins. In contrast, such VANC-related proteins were not found in any of the TIR-*MULE* members. Therefore, association between the VANC-related proteins and the absence of long TIRs is very tight. The non-TIR *MULE*s seem to keep VANC-related proteins during evolution.

While transposases of the MURA class are generally found in autonomous *MULE*s, other ORFs in *MULE*s tend to be diverse. Consistent with that, nucleotide divergence is higher in *vanC*-related genes than in *vanA*-related genes, especially between distant groups (Figures 7B and 8). However, that does not seem to be due to weaker constraint on the amino-acid sequence of the VANC-related proteins, because non-synonymous mutation rates are comparable between both families of genes and the overall high divergence seems to reflect the divergence in synonymous sites (Figure 8). The conserved amino-acid sequences in the VANC-related proteins suggest advantage in their functions, at least in short term.

Genome-wide effects of Hi transgene on DNA methylation

Hi transgene affects endogenous *Hi* sequence. We then examined the effect of *Hi* transgene genome-wide. DNA methy-

lation was examined, because that could be accessed relatively precisely using whole-genome bisulphite sequencing. In the whole-genome bisulphite sequencing, deep sequencing reads are mapped to the reference genome sequence. In order to reduce possible noise due to repetitive nature of TEs, we used only uniquely mapped reads; reads mapped to multiple loci were not used for the analyses. The analyses revealed that many of the *VANDAL21* members showed reduced DNA methylation in the transgenic line (Figure 9A and B; Supplementary Figures S12–S14; Supplementary Table S3). Interestingly, not only terminal regions but also internal regions were affected for both *Hi* and other *VANDAL21* copies (Figure 9B; Supplementary Figure S14). As is the case for the *Hi* sequence, non-CpG sites tend to be more affected than CpG sites. On the other hand, the demethylating effect was much less in the other TEs and genes (Figure 9A; Supplementary Figure S12), suggesting that the *trans*-acting effects of *Hi* are highly specific.

Table I Comparison of copy numbers per cluster between non-TIR and TIR *MULE*s

	#Seq[a]	#Cluster[b]	Seq/cluster	*t*
A. thaliana				
TIR *MULE*s	27	24 (21)	1.125	4.42
Non-TIR *MULE*s	143	34 (13)	4.206	$P<0.001$
A. lyrata				
TIR *MULE*s	85	39 (21)	2.179	2.38
Non-TIR *MULE*s	219	49 (20)	4.347	$P<0.02$

Analyses were performed using transposase genes. Therefore, copies without the conserved transposase gene are not included in the analyses. Details for the analyses are described in Materials and methods.
[a]Number of sequences analysed.
[b]Number of cluster with <0.1 *p*-distances. In the parentheses, number of clusters with only one sequence is shown.

Discussion

Trans-activation as a counteraction against genome defense by the host

Here, we report identification of an autonomously mobile copy of *MULE* that lacks long TIRs. Among three ORFs *Hi* contains, *vanA* encodes for a putative transposase conserved among other TEs. Most importantly, *vanC*, another ORF of *Hi*, plays a key role in the transcriptional activation of the other ORFs in *Hi*, and in mobilization of *Hi*. These *trans*-acting effects represent efficient means for counteracting DNA methylation and silencing by the host.

Importantly, the anti-silencing mechanism of *Hi* seems to function specifically, rather than globally (Figure 9). In contrast, some viruses have evolved mechanisms to globally inhibit RNA interference (RNAi)/post-transcriptional gene silencing (PTGS). RNAi/PTGS is an important mechanism for defense against viruses, and the global anti-silencing would facilitate proliferation of the viruses (Zamore, 2004; Bivalkar-Mehla *et al*, 2011). In contrast to the global anti-silencing mechanisms of these viruses, *Hi* seems to target related TEs specifically. The specific (rather than global) anti-silencing can be reasonable for a TE. If a TE has global anti-silencing mechanisms, such as genome-wide demethylation, then that would activate diverse TEs, reducing fitness of the host (Lippman *et al*, 2004; Tsukahara *et al*, 2012). Reduction of host fitness would be deleterious for survival of the TE itself, given that the TE is an obligatory intra-genomic parasite/symbiont. The strategy of a TE should be different from that of viruses, which can propagate horizontally away from damaged hosts.

Mechanisms for the trans-acting effects

VANC induces both transcriptional activation and loss of DNA methylation *in trans*. Genome-wide analyses of transgenic plants revealed that the *trans*-acting demethylation

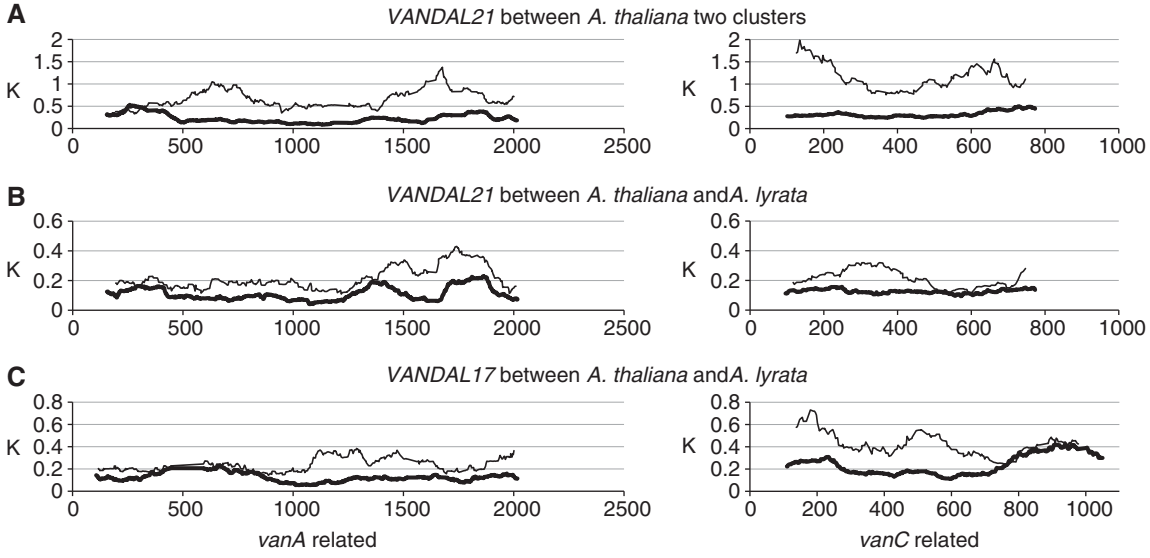

Figure 8 Sliding window plot analyses of *VANDAL21* and the most related family *VANDAL17*. (**A**) Divergence between two clusters (seven copies and three copies) of *VANDAL21* family in *A. thaliana*. (**B**) Divergence between *VANDAL21* copies in *A. thaliana* (three copies, which are orthologous to the *A. lyrata* copies) and *A. lyrata* (six copies). (**C**) Divergence between *VANDAL17* family in *A. thaliana* (four copies) and *A. lyrata* (three copies). Level of divergence for synonymous and non-synonymous sites in a 200-bp window was plotted in 1 bp intervals. Only coding sequences of complete structures were used. Thin lines and thick lines indicate synonymous and non-synonymous divergences, respectively.

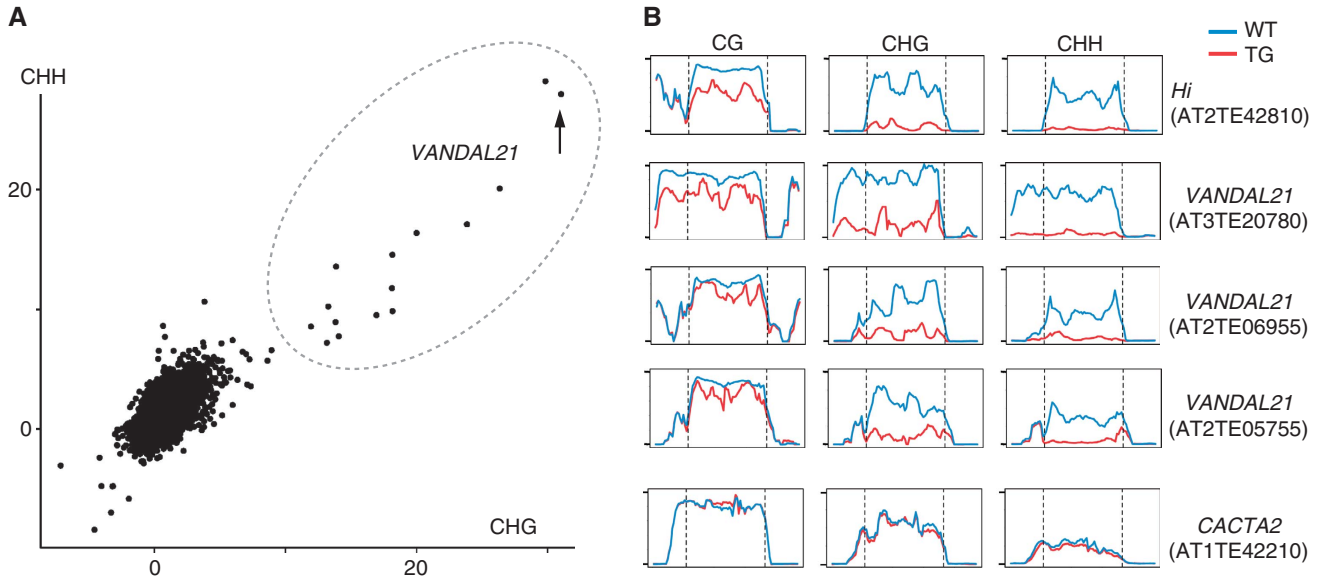

Figure 9 Demethylation of *VANDAL21* members induced by *Hi* transgene. (**A**) Effects of *Hi* transgene on DNA methylation in TEs. Changes in methylation at CpHpG sites and CpHpH sites are plotted. For each of them, significance of decrease in methylation was accessed by the value $(Mn/Cn - Mt/Ct)/(1/\sqrt{Cn} + 1/\sqrt{Ct})$, where *Mn*, *Cn*, *Mt* and *Ct* are methylated cytosine (*M*) and total cytosine (*C*) counts mapped for each TE in the non-transgenic (*n*) and transgenic (*t*) plants, respectively. Each of these values is shown in Supplementary Table S3, with the corresponding values for CpG sites. This figure contains 24 282 TEs plotted, while 6910 TEs are not plotted due to lack of mapped cytosine in one or more of the three contexts in non-transgenic or transgenic plant. The lack is mainly because we did not use reads mapped multiple loci. Some of the *VANDAL21* family members (surrounded by broken ellipse) showed most significant reduction for both CpHpG and CpHpH sites. The dot for *Hi* is indicated by an arrow. Similar analyses done on genes are shown in Supplementary Figure S12. (**B**) Effect of *Hi* transgene on DNA methylation across each of the *VANDAL21* members. Left and right terminals are shown by broken lines for each element. Each point represents proportion of methylated cytosine for a sliding window with seven fractions after separating each TE for 100 fractions. Right and left flanking regions are also analysed by the same conditions. Scale bars for CpG, CpHpG, and CpHpH sites in each panel indicate 1, 0.8, and 0.4, respectively. For some of the *VANDAL21* copies, reduced methylation in the terminal region is also confirmed by conventional bisulphite sequencing using primers within and flanking the TE (Supplementary Figure S13). Results of DNA methylation across six additional *VANDAL21* members are shown in Supplementary Figure S14. *CACTA2* is shown as a negative control.

occurs specifically in *Hi* and other *VANDAL21* members. How is the specific loss of methylation induced? In the case of *Tam3* transposon of snapdragon, loss of methylation is associated with binding of the transposase (Hashida *et al*, 2006). It would be informative to know localization of VANC protein in the genome.

Another possible pathway could be demethylation through transcription. Transcription can induce loss of methylation in lysine 9 of histone H3 (H3K9) through the function of histone demethylase IBM1 (Inagaki *et al*, 2010). The loss of H3K9 methylation induces loss of non-CpG methylation. That would account for the effect of *Hi* on non-CpG methylation in the internal regions of TEs (Figure 9; Supplementary Figure S14). Generally, DNA methylation in both CpG and non-CpG sites could be involved in silencing of TEs (Johnson *et al*, 2003; Kato *et al*, 2003). Considering that active/inactive states of TEs can be stabilized by positive feedback loops, possible interactions between transcription and DNA methylation at CpG and non-CpG sites would be important for understanding TE dynamics (Saze and Kakutani, 2011; Inagaki and Kakutani, 2013; further discussion in Supplementary Figure S15).

Role of VANC and loss of TIR

Non-TIR *MULE*s found within *A. thaliana* genome seem to be derived from ancestral TIR *MULE*s (Yu *et al*, 2000). Interestingly, evolution of non-TIR *MULE*s is tightly associated with the VANC-related proteins (Supplementary Figure S11). How has the transition from TIR type to non-TIR type of *MULE*s occurred? That could be due to loss of restraint to keep long TIRs, possibly reflecting evolution of transposition machinery. Despite degeneration of TIRs, most of the *Hi* excisions occurred in a manner to keep the original sequence before integration. That was found for both *Hi* mobilized in *ddm1* mutation (Supplementary Figure S3A) and by the *Hi* transgene (Supplementary Figure S3B). We could detect excision of endogenous *Hi* in Δ*C*-TG, but the efficiency tends to be low compared with the full-length TG (Figure 5A; Supplementary Figures S3C and S9). VANC might also have a role in efficient transposition with degenerated TIR. It is also possible that degeneration of the TIR had some advantage for the TE. One possible advantage of losing the TIR would be escape from siRNA-based silencing mechanisms. Long TIRs of *MULE*s are often associated with siRNA, and generation of siRNA might be less efficient in non-TIR *MULE*s. Irrespective of the range of functions, the VANC-related proteins are tightly associated with the non-TIR *MULE* lineages, and the efficient recent proliferations of these TEs (Figure 7A; Table I) may depend on these proteins.

Materials and methods

Plant materials

The *ddm1-1* mutant allele was used throughout, except for epi-RILs, which are originated from *ddm1-2* mutant. Details for self-pollination of *ddm1-1/ddm1-1* mutants and wild-type *DDM1/DDM1* siblings were described previously (Kakutani *et al*, 1996). Generation of epi-RILs is described in Johannes *et al* (2009). Mutant alleles used for experiments in Supplementary Figure S15 are those described in Sasaki *et al* (2012).

Identification of mobile VANDAL21 copies

Conditions for suppression PCR were described previously (Miura *et al*, 2001). To detect *de novo* insertions from whole-genome sequence data of self-pollinated *ddm1* plants (Tsukahara *et al*, 2012), reads containing terminal sequences of *VANDAL21* copies were selected first, and the flanking sequences were subsequently extracted from those reads. In both approaches, each of the *VANDAL21* copies can be distinguished by polymorphisms in the terminal regions. Raw sequence data for the self-pollinated *ddm1* plants were deposited in the DDBJ (DNA Data Bank of Japan) Sequence Read Archive (DRA; accession nos. DRA000420–000424).

DNA preparation and copy number quantification

DNA was extracted using DNeasy kit (QIAGEN). Copy number of *Hi* in the genome was quantified at region C1 (Figure 1) by quantitative PCR using Light Cycler 480 machine (Roche) and SYBR green I MasterMix (Roche) and normalized with signals for two single-copy loci, *AT5G13440* and *AT5G36220*. For this and all other experiments, sequences of primers used are listed in Supplementary Table S2.

Detecting excision of endogenous Hi

Excision of *Hi* was detected using nested PCR with the following conditions. First PCR: 94°C for 2 min, 25 cycles of (94°C for 30 s; 55°C for 30 s; 72°C for 30 s), and 72°C for 2 min. The products diluted to 20 times by H_2O were used for second PCR: 94°C for 2 min, 30 cycles of (94°C for 30 s; 55°C for 30 s; 72°C for 30 s), and 72°C for 2 min. The sequence after excision of endogenous *Hi* was determined after PCR and subsequent cloning by TA-cloning kit (Invitrogen).

DNA methylation analyses

Conventional bisulphite sequence analysis was performed as described previously (Tsukahara *et al*, 2009). For genome-wide bisulphite sequencing analyses, sequencing libraries (insert size: 300–400 bp) were prepared using TruSeq DNA LT Sample Prep Kit (Illumina) and subjected to bisulphite conversion using MethylCode Bisulfite Conversion Kit (Life Technologies). Bisulphite-treated DNA molecules were PCR amplified with 10 cycles using KAPA HiFi HotStart Uracil+ ReadyMix (2 ×) (Kapa Biosystems) and purified with Agencourt AMPure XP (Beckman Coulter). Conditions of the sequencing are as described previously (Tsukahara *et al*, 2012). Raw sequence data were deposited in the DDBJ (DNA Data Bank of Japan) Sequence Read Archive (DRA; accession nos. DRA001060 and DRA001061). Reads were mapped to the reference genome (Release 10 of the Arabidopsis Information Resources) using the Bowtie alignment algorithm (Langmead *et al*, 2009) with conditions described by Chen *et al* (2010). Only uniquely mapped reads were used; reads mapped more than once were not used. Annotation of TEs is obtained from TAIR (http://www.arabidopsis.org/), which is based on Buisine *et al* (2008).

Measurement of DNA methylation was also performed by McrBC digestion and subsequent quantitative PCR as described previously (Teixeria *et al*, 2009). McrBC (New England Biolabs) digestion was performed on 200 ng of genomic DNA. Digested and undigested DNA samples were quantified as described above. The methylation status was estimated by the loss of long DNA after McrBC digestion.

Transcription analysis

Total RNA was isolated by Promega SV Total RNA Isolation System (cat. #Z3100). Reverse transcription reaction was performed using Takara RNA PCR Kit (RR019A) following the manufacturer's instructions. Oligo dT-Adaptor primer was used to reverse transcribe predicted products of three coding genes of *Hi*. GAPC was used as a control. qRT–PCR was performed using SYBR Premix Ex Taq II (Takara) on Thermal Cycler Dice_Real Time System TP800 (Takara), with the following conditions; 95°C for 30′, (95°C for 5′, 60°C for 30′ and 72°C for 30′) for 40 times. The *UBC* gene (*At5g25760*) was used as an internal control.

Transgene construction

Full-length *Hi* was recovered by PCR and cloned into vector PZP2H-lac (Fuse *et al*, 2001). In most constructs, silent mutations were introduced for each of the three ORFs, so that transcripts from the transgene and endogenous copies could be distinguished between (Figure 1). Transgenes with deletion in each of the three ORFs were generated by PCR using the full-length *Hi* as the template. Primer sequences for generating these constructs are shown in Supplementary Table S2.

Molecular evolutionary analyses

BLAST searches of the *A. lyrata* genome were conducted with *A. thaliana MULE* family sequences as the query against assembled genomes by Phytozome ver 8.0 (Goodstein *et al*, 2012). A conserved transposase region, analysed by Yu *et al* (2000), was used for estimation of entire *MULE* family phylogeny. The neighbour-joining trees were constructed by the *p*-distance in MEGA 5 (Tamura *et al*, 2011). To analyse the proliferation rate, copy numbers in recently proliferated clusters were estimated. The *p*-distance of 0.1 was used as a threshold value to classify each copy to clusters and then numbers of copies in each cluster were counted. Average numbers of copies per cluster were compared between non-TIR MULE families and TIR MULE families by *t*-test. The sliding window analyses of synonymous and non-synonymous distances between subcluster and between species for *VANDAL21* and *VANDAL17* families were conducted by DnaSP ver. 5 (Librado and Rozas, 2009). Conserved domain was searched by NCBI conserved domain search site (Marchler-Bauer *et al*, 2011; http://www.ncbi.nlm.nih.gov/Structure/cdd/wrpsb.cgi).

Supplementary data

Supplementary data are available at *The EMBO Journal* Online (http://www.embojournal.org).

Acknowledgements

We thank Akiko Terui and Kazuya Takashima for technical assistance. Special thanks to Damon Lisch for valuable advice about *Mutator* and TIR, Yasuhiko Sekine for transposition mechanisms, and Yasushi Hiromi for comments on the manuscript. Supported by grants from Mitsubishi Foundation (to TK), Takeda Science Foundation (to TK), Japanese Ministry of Education, Culture, Sports, Science and Technology (19207002 and 19060014, to TK), Systems Functional Genetics Project of the Transdisciplinary Research Integration Center, ROIS, Japan (to AT, AF, YT, and TK), the Agence Nationale de la Recherche (Project EPIMOBILE, NT09_501422 to VC), and the European Union Network of Excellence Epigenesys (to VC). ME was supported by a PhD studentship from the French Ministry of Research.

Author contributions: AK designed and performed sequence analyses (Figures 7 and 8; Supplementary Figures S10 and S11). ME and VC designed and performed experiments using epi-RILs (Figure 3). YF, TI, AT, AF, YT, and TK designed, performed, and analysed whole-genome bisulphite sequencing and genome re-sequencing experiments. YF, YT, and TK designed and performed all other experiments. YF and TK wrote the paper with incorporating comments from other authors.

Conflict of interest

The authors declare that they have no conflict of interest.

References

Bivalkar-Mehla S, Vakharia J, Mehla R, Abreha M, Kanwar JR, Tikoo A, Cahuhan A (2011) Viral RNA silencing suppressors (RSS): novel strategy of viruses to ablate the host RNA interference (RNAi) defense system. *Virus Res* **155:** 1–9

Brettell RI, Dennis ES (1991) Reactivation of a silent Ac following tissue culture is associated with heritable alterations in its methylation. *Mol Gen Genet* **229:** 365–372

Brown WE, Robertson DS, Bennetzen JL (1989) Molecular analysis of multiple Mutator-derived alleles of the Bronze locus of maize. *Genetics* **122:** 439–445

Brown J, Sundaresan V (1992) Genetic study of the loss and restoration of Mutator transposon activity in maize: evidence against dominant-negative regulator associated with loss of activity. *Genetics* **130:** 889–898

Buisine N, Quesneville H, Colot V (2008) Improved detection and annotation of transposable elements in sequenced genomes using multiple reference sequence sets. *Genomics* **91:** 467–475

Chandler VL, Walbot V (1986) DNA modification of a maize transposable element correlates with loss of activity. *Proc Natl Acad Sci USA* **83:** 1767–1771

Chen PY, Cokus SJ, Pellegrini M (2010) BS Seeker: precise mapping for bisulfite sequencing. *BMC Bioinformatics* **11:** 203

Colomé-Tatché M, Cortijo S, Wardenaar R, Morgado L, Lahouze B, Sarazin A, Etcheverry M, Martin A, Feng S, Duvernois-Berthet E, Labadie K, Wincker P, Jacobsen SE, Jansen RC, Colot V & Johannes F (2012) Features of the Arabidopsis recombination landscape resulting from the combined loss of sequence variation and DNA methylation. *Proc Natl Acad Sci USA* **109:** 16240–16245

Cui H, Fedoroff NV (2002) Inducible DNA demethylation mediated by the maize Suppressor-mutator transposon-encoded TnpA protein. *Plant Cell* **14:** 2883–2899

Dietrich CR, Cui F, Packila ML, Li J, Ashlock DA, Nikolau BJ, Schnable PS (2002) Maize Mu transposons are targeted to the 5′ untranslated region of the gl8 gene and sequences flanking Mu target-site duplications exhibit nonrandom nucleotide composition throughout the genome. *Genetics* **160:** 697–716

Eisen JA, Benito MI, Walbot V (1994) Sequence similarity of putative transposases links the maize Mutator autonomous element and a group of bacterial insertion sequences. *Nucleic Acids Res* **22:** 2634–2636

Fedoroff N (1996) Epigenetic regulation of the maize *Spm* transposable element. In *Epigenetic Mechanisms of Gene Regulation*, Riggs A, Martienssen R, Russo V (eds), pp 575–592. Cold Spring Harbor, New York: Cold Spring Harbor Laboratory Press

Fuse T, Sasaki T, Yano M (2001) Ti-plasmid vectors useful for functional analysis of rice genes. *Plant Biotechnol* **18:** 219–222

Goodstein DM, Shu S, Howson R, Neupane R, Hayes RD, Fazo J, Mitros T, Dirks W, Hellsten U, Putnam N, Rokhsar DS (2012) Phytozome: a comparative platform for green plant genomics. *Nucleic Acids Res* **40:** D1178–D1186

Hashida S, Uchiyama T, Martin C, Kishima Y, Sano Y, Mikami T (2006) The temperature dependent change in Methylation of the Antirrhinum transposon Tam3 is controlled by the activity of its transposase. *Plant Cell* **18:** 104–118

Hardeman KJ, Chandler VL (1989) Characterization of bz1 mutants isolated from mutator stocks with high and low numbers of Mu1 elements. *Dev Genet* **10:** 460–472

Hoen DR, Park KC, Elrouby N, Yu Z, Mohabir N, Cowan RK, Bureau TE (2006) Transposon-mediated expansion and diversification of a family of ULP-like genes. *Mol Biol Evol* **23:** 1254–1268

Inagaki S, Miura A, Nakamura K, Lu F, Cui X, Cao X, Kimura H, Saze H, Kakutani T (2010) Autocatalytic differentiation of epigenetic modifications within the Arabidopsis genome. *EMBO J* **29:** 3496–3506

Inagaki S, Kakutani T (2013) What triggers differential DNA methylation of genes and TEs: contribution of body methylation? *Cold Spring Harb Symp Quant Biol* **77:** 155–160

Jiang N, Bao Z, Zhang X, Eddy SE, Wessler SR (2004) Pack-MULE transposable elements mediate gene evolution in plants. *Nature* **431:** 569–573

Johnson L, Cao X, Jacobsen S (2003) Interplay between two epigenetic marks. DNA methylation and histone H3 lysine 9 methylation. *Curr Biol* **12:** 1360–1367

Johannes F, Porcher E, Teixeira FK, Saliba-Colombani V, Simon M, Agier N, Bulski A, Albuisson J, Heredia F, Audigier P, Bouchez D, Dillmann C, Guerche P, Hospital F, Colot V (2009) Assessing the impact of transgenerational epigenetic variation on complex traits. *PLoS Genet* **5:** e1000530

Kakutani T, Jeddeloh JA, Flowers SK, Munakata K, Richards EJ (1996) Developmental abnormalities and epimutations associated with DNA hypomethylation mutations. *Proc Natl Acad Sci USA* **93:** 12406–12411

Kato M, Miura A, Bender J, Jacobsen SE, Kakutani T (2003) Role of CG and non-CG methylation in immobilization of transposons in Arabidopsis. *Curr Biol* **13:** 421–426

Langmead B, Trapnell C, Pop M, Salzberg SL (2009) Ultrafast and memory-efficient alignment of short DNA sequences to the human genome. *Genome Biol* **10:** R25

Le QH, Wright S, Yu Z, Bureau T (2000) Transposon diversity in Arabidopsis thaliana. *Proc Natl Acad Sci USA* **97:** 7376–7381

Librado P, Rozas J (2009) DnaSP v5: a software for comprehensive analysis of DNA polymorphism data. *Bioinformatics* **25:** 1451–1452

Lippman Z, Gendrel AV, Black M, Vaughn MW, Dedhia N, McCombie WR, Lavine K, Mittal V, May B, Kasschau KD, Carrington JC, Doerge RW, Colot V, Martienssen R (2004) Role of transposable elements in heterochromatin and epigenetic control. *Nature* **430:** 810–813

Liu S, Yeh CT, Ji T, Ying K, Wu H, Tang HM, Fu Y, Nettleton D, Schnable PS (2009) Mu transposon insertion sites and meiotic recombination events co-localize with epigenetic marks for open chromatin across the maize genome. *PLoS Genet* **5:** e1000733

Lisch D (2002) Mutator transposons. *Trends Plant Sci* **7:** 498–504

Lisch D, Chomet P, Freeling M (1995) Genetic characterization of the Mutator system in maize: behavior and regulation of Mu transposons in a minimal line. *Genetics* **139:** 1777–1796

Lisch D, Girard L, Donlin M, Freeling M (1999) Functional analysis of deletion derivatives of the maize transposon MuDR delineates roles for the MURA and MURB proteins. *Genetics* **151:** 331–341

Marchler-Bauer A, Lu S, Anderson JB, Chitsaz F, Derbyshire MK, DeWeese-Scott C, Fong JH, Geer LY, Geer RC, Gonzales NR, Gwadz M, Hurwitz DI, Jackson JD, Ke Z, Lanczycki CJ, Lu F, Marchler GH, Mullokandov M, Omelchenko MV, Robertson CL *et al* (2011) CDD: a Conserved Domain Database for the functional annotation of proteins. *Nucleic Acids Res* **39,** (Database issue) D225–D229

Martienssen R (1996) Epigenetic silencing of *Mu* transposable elements in maize. In *Epigenetic Mechanisms of Gene Regulation*, Riggs A, Martienssen R, Russo V (eds), pp 593–608. Cold Spring Harbor, New York: Cold Spring Harbor Laboratory Press

Martienssen R, Baron A (1994) Coordinate suppression of mutations caused by Robertson's mutator transposons in maize. *Genetics* **136:** 1157–1170

McClintock B (1951) Chromosome organization and genic expression. *Cold Spring Harbor Symp Quant Biol* **16:** 13–47

McClintock B (1958) The suppressor-mutator system of control of gene action in maize. *Carnegie Institution of Washington Year Book* Vol. 57: 415–429

Mirouze M, Reinders J, Bucher E, Nishimura T, Schneeberger K, Ossowski S, Cao J, Weigel D, Paszkowski J, Mathieu O (2009) Selective epigenetic control of retrotransposition in Arabidopsis. *Nature* **461:** 427–430

Miura A, Yonebayashi S, Watanabe K, Toyama T, Shimada H, Kakutani T (2001) Mobilization of transposons by a mutation abolishing full DNA methylation in Arabidopsis. *Nature* **411:** 212–214

Saze H, Kakutani T (2011) Differentiation of epigenetic modifications between transposons and genes. *Curr Opin Plant Biol* **65:** 589–599

Sasaki T, Kobayashi A, Saze H, Kakutani T (2012) RNAi-independent *de novo* DNA methylation revealed in Arabidopsis mutants of chromatin remodeling gene DDM1. *Plant J* **70:** 750–758

Schläppi M, Raina R, Fedoroff N (1994) Epigenetic regulation of the maize Spm transposable element: novel activation of a methylated promoter by TnpA. *Cell* **77:** 427–437

Schläppi M, Raina R, Fedoroff N (1996) A highly sensitive plant hybrid protein assay system based on the Spm promoter and TnpA protein for detection and analysis of transcription activation domains. *Plant Mol Biol* **32:** 717–725

Singer T, Yordan C, Martienssen RA (2001) Robertson's Mutator transposons in A. thaliana are regulated by the chromatin-remodeling gene Decrease in DNA Methylation (DDM1). *Genes Dev* **15:** 591–602

Talbert LE, Chandler VL (1988) Characterization of a highly conserved sequence related to *mutator* transposable elements in maize. *Mol Biol Evol* **5:** 519–529

Tamura K, Peterson D, Peterson N, Stecher G, Nei M, Kumar S (2011) MEGA5: Molecular evolutionary genetics analysis using maximum likelihood, evolutionary distance, and maximum parsimony methods. *Mol Biol Evol* **28:** 2731–2739

Teixeria FK, Heredia F, Sarazin A, Roudier F, Boccara M, Ciaudo C, Cruaud C, Poulain J, Berdasco M, Fraga MF, Voinnet O, Wincker P, Esteller M, Colot V (2009) A role for RNAi in the selective correction of DNA methylation defects. *Science* **323:** 1600–1604

Tsukahara S, Kobayashi A, Kawabe A, Mathieu O, Miura A, Kakutani T (2009) Bursts of retrotransposition reproduced in Arabidopsis. *Nature* **461:** 423–426

Tsukahara S, Kawabe A, Kobayashi A, Ito T, Aizu T, Shin-i T, Toyoda A, Fujiyama A, Tarutani Y, Kakutani T (2012) Centromere-targeted *de novo* integrations of an LTR retrotransposon of Arabidopsis lyrata. *Genes Dev* **26:** 705–713

Wicker T (2007) A unified classification system for eukaryotic transposable elements. *Nat Rev Genet* **8:** 973–982

Yu Z, Wright SI, Bureau TE (2000) Mutator-like elements in Arabidopsis thaliana. Structure, diversity and evolution. *Genetics* **156:** 2019–2031

Zamore PD (2004) Plant RNAi: How a viral silencing suppressor inactivate siRNA. *Curr Biol* **14:** R198–R200